

1-1-2010

Direct measurement of electric-field-induced birefringence in a polymer-stabilized blue-phase liquid crystal composite

Jin Yan

University of Central Florida

Meizi Jiao

University of Central Florida

Linghui Rao

University of Central Florida

Shin-Tson Wu

University of Central Florida

Find similar works at: <https://stars.library.ucf.edu/facultybib2010>

University of Central Florida Libraries <http://library.ucf.edu>

This Article is brought to you for free and open access by the Faculty Bibliography at STARS. It has been accepted for inclusion in Faculty Bibliography 2010s by an authorized administrator of STARS. For more information, please contact STARS@ucf.edu.

Recommended Citation

Yan, Jin; Jiao, Meizi; Rao, Linghui; and Wu, Shin-Tson, "Direct measurement of electric-field-induced birefringence in a polymer-stabilized blue-phase liquid crystal composite" (2010). *Faculty Bibliography 2010s*. 968.

<https://stars.library.ucf.edu/facultybib2010/968>

Direct measurement of electric-field-induced birefringence in a polymer-stabilized blue-phase liquid crystal composite

Jin Yan, Meizi Jiao, Linghui Rao, and Shin-Tson Wu*

College of Optics and Photonics, University of Central Florida, Orlando, Florida 32816, USA
*swu@mail.ucf.edu

Abstract: We demonstrate a method to directly measure the electric-field-induced birefringence of a polymer-stabilized blue-phase liquid crystal (PS-BPLC) composite. The induced birefringence follows the extended Kerr effect well and is approximately 3X the ordinary refractive index change. The measured data are validated by comparing the simulated and measured voltage-dependent transmittance with an in-plane switching cell. The impact of these results to the material optimization of emerging BPLC displays is discussed.

©2010 Optical Society of America

OCIS codes: (160.3710) Liquid crystals; (290.3030) Index measurements; (260.1440) Birefringence

References and links

1. H. Kikuchi, M. Yokota, Y. Hisakado, H. Yang, and T. Kajiyama, "Polymer-stabilized liquid crystal blue phases," *Nat. Mater.* **1**(1), 64–68 (2002).
2. S. W. Choi, S. I. Yamamoto, Y. Haseba, H. Higuchi, and H. Kikuchi, "Optically isotropic-nanostructured liquid crystal composite with high Kerr constant," *Appl. Phys. Lett.* **92**(4), 043119 (2008).
3. Z. Ge, S. Gauza, M. Jiao, H. Xianyu, and S. T. Wu, "Electro-optics of polymer-stabilized blue phase liquid crystal displays," *Appl. Phys. Lett.* **94**(10), 101104 (2009).
4. Z. Ge, L. Rao, S. Gauza, and S. T. Wu, "Modeling of blue phase liquid crystal displays," *J. Display Technol.* **5**(7), 250–256 (2009).
5. L. Rao, Z. Ge, S. T. Wu, and S. H. Lee, "Low voltage blue-phase liquid crystal displays," *Appl. Phys. Lett.* **95**(23), 231101 (2009).
6. M. Jiao, Y. Li, and S. T. Wu, "Low voltage and high transmittance blue-phase liquid crystal displays with corrugated electrodes," *Appl. Phys. Lett.* **96**(1), 011102 (2010).
7. K. M. Chen, S. Gauza, H. Xianyu, and S. T. Wu, "Submillisecond gray-level response time of a polymer-stabilized blue-phase liquid crystal," *J. Display Technol.* **6**(2), 49–51 (2010).
8. S. Meiboom, J. P. Sethna, W. P. Anderson, and W. F. Brinkman, "Theory of the blue phase cholesteric liquid crystals," *Phys. Rev. Lett.* **46**(18), 1216–1219 (1981).
9. J. Kerr, "A new relation between electricity and light: Dielectric media birefringent," *Philos. Mag.* **50**, 337–348 (1875).
10. P. R. Gerber, "Electro-optical effects of a small-pitch blue-phase system," *Mol. Cryst. Liq. Cryst. (Phila. Pa.)* **116**(1), 197–206 (1985).
11. Y. Haseba, H. Kikuchi, T. Nagamura, and T. Kajiyama, "Large electro-optic Kerr effect in nanostructured chiral liquid-crystal composites over a wide-temperature range," *Adv. Mater.* **17**(19), 2311–2315 (2005).
12. J. Yan, H. C. Cheng, S. Gauza, Y. Li, M. Jiao, L. Rao, and S. T. Wu, "Extended Kerr effect of polymer-stabilized blue-phase liquid crystals," *Appl. Phys. Lett.* **96**(7), 071105 (2010).
13. J. Li, G. Baird, Y. H. Lin, H. Ren, and S. T. Wu, "Refractive-index matching between liquid crystals and photopolymers," *J. Soc. Inf. Disp.* **13**(12), 1017–1026 (2005).
14. G. L. Cloud, *Optical Methods of Engineering Analysis* (Cambridge, New York, 1998).

1. Introduction

Polymer-stabilized blue phase liquid crystal (PS-BPLC) [1–6] is emerging as next-generation display technology due to its revolutionary features, such as no need for alignment layer, submillisecond gray-to-gray response time [7], and inherently wide viewing angle. According to Meiboom's model [8], BPLCs are comprised of double twist cylinders. It appears to be optically isotropic since the molecules can be regarded as randomly distributed. Applying an electric field causes the molecules to be reoriented along the electric field direction. As a

result, birefringence is induced. Macroscopically this optically isotropic-to-anisotropic transition can be treated as Kerr effect [9, 10]. The refractive index difference along and perpendicular to the electric field is called induced birefringence. This electric field-induced birefringence needs to be determined in order to better describe the electro-optical properties of the BPLC device. To measure the induced birefringence, two methods have been introduced [11, 12]. In Ref [11], a cell with two planar ITO (indium tin oxide) substrates was filled with PS-BPLC and was tilted by 45° to obtain an effective birefringence. This effective birefringence was then converted to the birefringence by a factor. Michelson interferometer was also employed to measure the induced birefringence [12]. However, both methods used some assumptions while converting the measured value to the induced birefringence.

In this paper, we develop experimental methods to directly measure the refractive indices parallel and perpendicular to the electric field, which lead to induced birefringence. No assumption is made during data processing. The electric field-induced birefringence follows well the extended Kerr effect described in Ref [12]. We further compare the measured voltage-dependent transmittance with simulation result to validate our obtained data. Good agreement between simulation and experiment is found. These measurement methods open a gateway for quantitatively evaluating the induced birefringence of a BPLC composite which, in turn, helps the development of BPLC materials with a large induced birefringence for lowering the operation voltage of display devices.

2. Experiment and theoretical analysis

The PS-BPLC employed in this study is a mixture comprising of nematic LC (48.6% Merck BL038), chiral dopants (20.2% Merck CB15 and 6% ZLI-4572) and monomers (10% EHA and 15.2% RM257). A small drop of the mixture was put on the main prism of an Abbe refractometer and covered by a lighting glass, as shown in Fig. 1 [13]. The lighting glass was used to compensate for the weak light since the BPLC layer is thin. The refractive index of the lighting glass is 1.6198, higher than that of the mixture. The lighting glass was pressed to get rid of bubbles in the BPLC layer. We controlled the temperature of the main prism at 45°C and cured the sample with UV light at $1\text{ mW}/\text{cm}^2$ for 30 min.

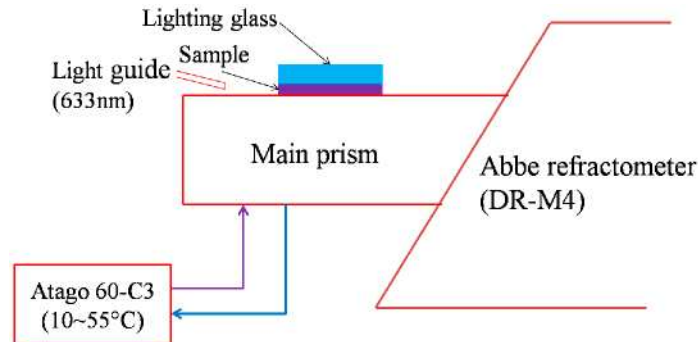


Fig. 1. Abbe refractometer for measuring the refractive index of PS-BPLC in voltage-off state

After UV curing, the sample was cooled down to room temperature ($\sim 23^\circ\text{C}$). By adjusting the height and angle of the light guide, we observed a clear boundary line through the eyepiece. The position of this line was adjusted to make it passing through the cross hairs and the measured refractive index was $n_i = 1.5878$.

The same mixture was also sandwiched between two ITO glass substrates with an $8\text{-}\mu\text{m}$ cell gap. The sample was UV cured under the same condition as the one on the Abbe refractometer. We used Michelson interferometer to measure the change of refractive indices (δn) perpendicular to the electric field. The PS-BPLC cell was placed in one arm and was driven by a 1 kHz square-wave voltage. The ordinary refractive index change under an electric field is written as follows:

$$\delta n(E) = n_i - n_o(E). \quad (1)$$

Here, n_i is the refractive index at voltage-off state, $n_o(E)$ is the field dependent refractive index perpendicular to the electric field. Since we have obtained n_i from Abbe refractometer, $n_o(E)$ can be calculated from Eq. (1).

To find the extraordinary refractive index of PS-BPLC, Senarmont method [14] was employed. The optical setup is shown in Fig. 2. The angles indicate the azimuthal angles of the transmission axes (for the polarizer and analyzer) or fast axes (for the sample and $\lambda/4$ plate). The PS-BPLC cell is tilted by an angle of θ to introduce phase retardation.

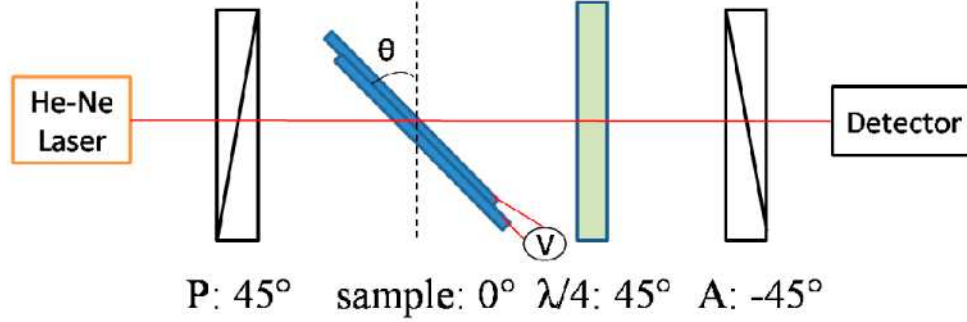


Fig. 2. Optical setup for Senarmont method. P: Polarizer, $\lambda/4$: quarter-wave plate, A: analyzer. The angle indicates the azimuthal angle of the transmission axis (for P and A) or fast axis (for sample and $\lambda/4$ plate).

The change of polarization state can be explained using Jones Matrix method. Since the transmission axis of the polarizer is 45° to the horizontal axis, the input field $E_{in} = \begin{bmatrix} \cos 45^\circ \\ \sin 45^\circ \end{bmatrix}$.

After passing through the $\lambda/4$ plate, the output field can be denoted as:

$$E_{out} = W(\pi/2)R(45^\circ)W(\Gamma)E_{in}, \quad (2)$$

where $W(\Gamma) = \begin{bmatrix} e^{-j\frac{\Gamma}{2}} & 0 \\ 0 & e^{j\frac{\Gamma}{2}} \end{bmatrix}$, $R(\phi) = \begin{bmatrix} \cos \phi & \sin \phi \\ -\sin \phi & \cos \phi \end{bmatrix}$, Γ is the phase retardation introduced

by the PS-BPLC sample. The x-y coordinates of output field are rotated by 45° so that they coincide with the axes of the $\lambda/4$ plate. Substituting W and R functions into Eq. (2) with the

given matrixes leads to $E_{out} = \begin{bmatrix} \cos \frac{\Gamma}{2} \\ \sin \frac{\Gamma}{2} \end{bmatrix}$. This output light is linearly polarized and can be

blocked by rotating the analyzer with an angle $\alpha = \Gamma/2$.

In the voltage-off state, the PS-BPLC cell is optically isotropic and does not introduce any phase retardation. The fast axis of the $\lambda/4$ plate coincides with the transmission axis of the polarizer, thus the polarization state does not change. Since the polarizer and the analyzer are crossed, the linearly polarized light is absorbed by the analyzer. As a voltage is applied to the sample, the introduced phase retardation has following form:

$$\Gamma(E) = \frac{2\pi}{\lambda} n_o(E) d \left[\sqrt{1 - \frac{\sin^2 \theta}{n_e^2(E)}} - \sqrt{1 - \frac{\sin^2 \theta}{n_o^2(E)}} \right]. \quad (3)$$

In Eq. (3), d is the cell gap and λ is the wavelength of the laser beam. For a given voltage, this phase retardation is measured at different incident angles and $n_e(E)$ is obtained through fitting.

3. Results and discussion

Figure 3 shows Δn_{eff} at 140 V_{rms} for different incident angles. Here we define

$$\Delta n_{eff}(E) = \frac{\lambda \Gamma(E)}{2\pi d} = n_o(E) \left(\sqrt{1 - \frac{\sin^2 \theta}{n_e^2(E)}} - \sqrt{1 - \frac{\sin^2 \theta}{n_o^2(E)}} \right). \quad (4)$$

The red curve is the fitting using Eq. (4) in which n_e is the fitting parameter, while $n_o = 1.5576$ was obtained from the Abbe and Michelson measurements through Eq. (1). Through fitting, we get $n_e = 1.6344$ at V=140 V_{rms}.

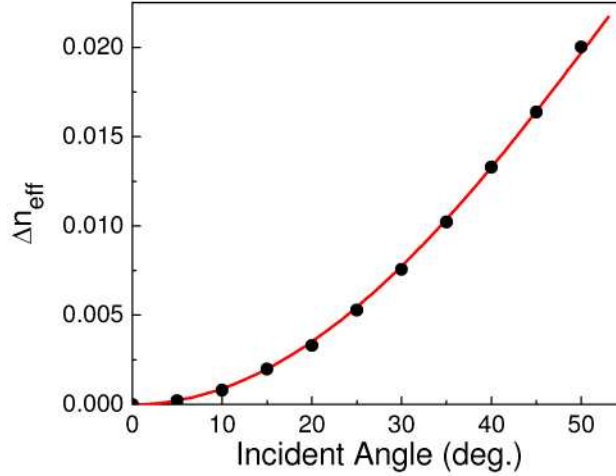


Fig. 3. Measured effective birefringence at different incident angles (circle) at V=140 V_{rms} and the fitting curve (red line) using Eq. (4). $\lambda=633$ nm and T=23°C.

The same fitting process was carried out at other voltages. Figure 4(a) shows the obtained n_o and n_e at different electric fields and Fig. 4(b) shows the induced birefringence obtained from $n_e - n_o$. In the low field region, conventional Kerr effect holds. The induced birefringence is linearly proportional to E^2 , where E is the electric field intensity. As the electric field increases, the induced birefringence gradually saturates and deviates from Kerr effect. This phenomenon was called extended Kerr effect [12]. In the extended Kerr effect, the convergence model was given by:

$$\Delta n = \Delta n_{sat} \left(1 - \exp \left[- \left(\frac{E}{E_s} \right)^2 \right] \right), \quad (5)$$

where Δn_{sat} stands for the saturated refractive index change and E_s represents the saturation field. The red curve in Fig. 4(b) is the fitting using Eq. (5). The parameters obtained through fitting are $\Delta n_{sat}=0.0873$ and $E_s = 12.15$ V/ μm . The Kerr constant under low field approximation is 0.93 nm/V².

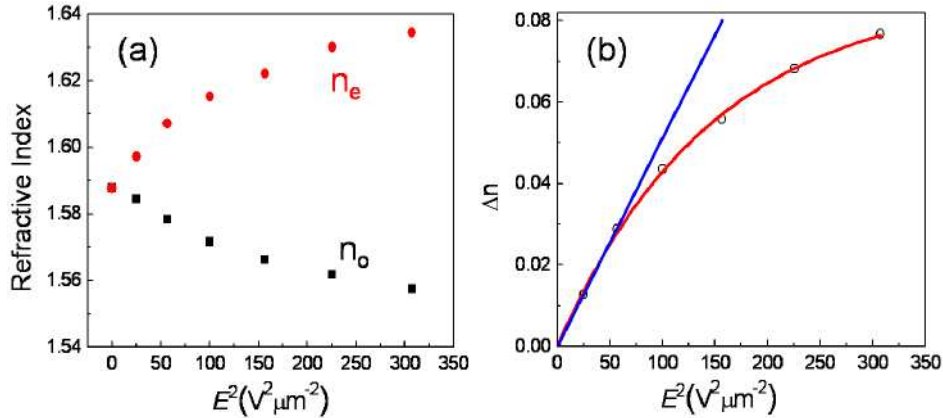


Fig. 4. (a) Electric field dependent ordinary refractive index (black squares) and extraordinary refractive index (red circles); (b) induced birefringence (circles), linear fitting in the low field region (blue straight line) and fitting using Eq. (5) (red curve). $\lambda=633$ nm and $T\sim 23^\circ\text{C}$.

The ratio of Δn to δn is plotted in Fig. 5. In previous study, we assumed that the average refractive index keeps constant at any electric field [12]. With this assumption, the induced birefringence Δn is related to δn by a factor of three. This ratio of three is within the error bar below $80 V_{\text{rms}}$. However, above $80 V_{\text{rms}}$ the ratio of Δn to δn slightly deviates from three. The underlying physical mechanism is still unclear, but one possible reason is that at high field the induced birefringence is not only due to the local reorientation of molecules, but lattice distortion could also come into play.

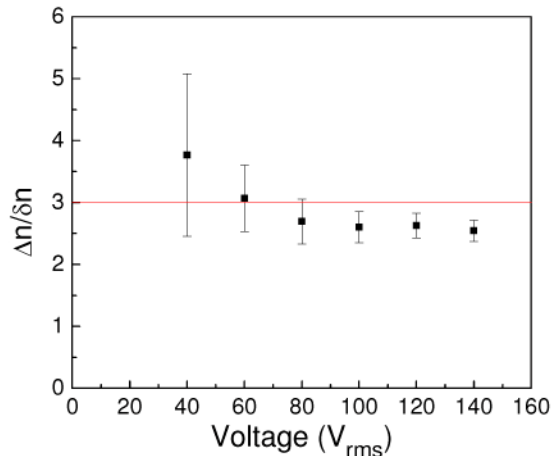


Fig. 5. Ratio of Δn to δn . The assumption ($\Delta n / \delta n = 3$) is shown in red line.

To validate our data, we filled an in-plane switching (IPS) cell with the same material and measured the voltage-dependent transmittance (VT) curve of this PS-BPLC device. The IPS cell has a cell gap of $7.5 \mu\text{m}$ with $10\text{-}\mu\text{m}$ electrode width and $10\text{-}\mu\text{m}$ electrode gap. Meanwhile, we incorporated Eq. (5) into our simulation program [6] and used the experimental data extrapolated from Fig. 4(b) to calculate the VT curve of this device.

Figure 6 shows the comparison of the experimental data with the simulation result. Since this IPS cell also behaves as a phase grating, it exhibits diffraction effects and this diffraction effect is also voltage dependent. To eliminate the influence of diffraction, we measured the VT curves under two crossed polarizers and two parallel polarizers, respectively. Only the intensity of zeroth order is recorded by the detector. The VT curve under two crossed polarizers is normalized to the summation of these two VT curves. This normalized VT curve

was again normalized to one in order to compare with the simulation result. Good agreement was obtained.

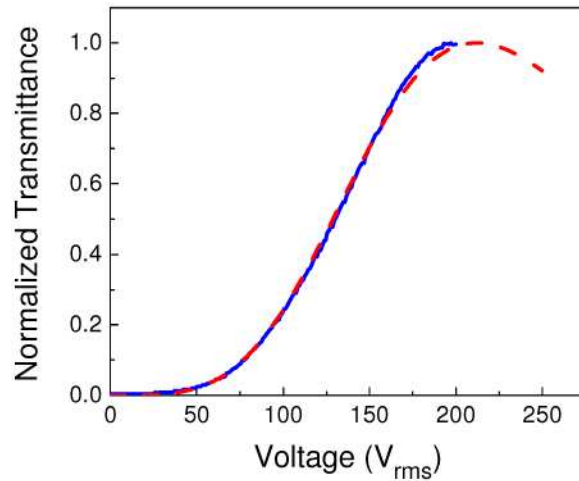


Fig. 6. Comparison of experimental data (solid blue line) of an IPS cell with simulation results (dashed red lines). $\lambda = 633$ nm and $T \sim 23^\circ\text{C}$.

4. Conclusion

We have demonstrated a method to directly measure the Kerr effect-induced ordinary and extraordinary refractive indices of a polymer-stabilized blue-phase liquid crystal composite. The electric-field-induced birefringence was further obtained. The induced birefringence follows well the extended Kerr effect and is approximately 3X the ordinary refractive index change. We further incorporated the measured data into our simulation program to predict the VT curve of an IPS display device. Good agreement was obtained between the simulation result and experimental data. This method provides unambiguous determination on the induced birefringence of a PS-BPLC composite. The obtained data will serve as useful guidelines for designing new BPLC materials with high Δn_{sat} and low E_s . These materials play a key role for lowering the operation voltage of BPLC display devices.

The authors are indebted to S. Gauza, Y. Li and H. C. Cheng for useful discussions and AFOSR for partial financial support under Contract No. FA95550-09-1-0170.